Appl. Magn. Reson. 12, 449–464 (1997)

Applied Magnetic Resonance

Quantitative Time-Resolved EPR CIDEP Study of the Photodecomposition of *trans*-Azocumene in Solution

A. N. Savitsky and H. Paul

Physikalisch-Chemisches Institut, Universität Zürich, Zürich, Switzerland

Received January 31, 1997

Abstract. The cumyl radical system, which is created after laser flash irradiation of *trans*-azocumene in benzene solution at room temperature, is investigated using time-resolved EPR spectroscopy. From the quantitative analysis of EPR time-profiles at different microwave powers the spin relaxation times $T_1 = 3.5 \pm 0.3$ μs and $T_2 = 2.5 \pm 0.1$ μs are evaluated as well as the magnitude of the chemically induced electron polarization (CIDEP), which is generated by the radical pair mechanism (RPM). The geminate RPM polarization is found to be considerably smaller than the F-pair one, 32 ± 2 and 48 ± 5 in units of the Boltzmann polarization, respectively. This is attributed to an initial radical separation in the geminate pair, caused by the cleavage reaction. Besides cleavage, the photoexcited *trans*-azocumene also decays via isomerization to the thermally unstable *cis*-isomer, the lifetime of which is found to be 14 ± 3 μs at 293 K in benzene, three times longer than in cyclohexane. The quantum yield of free radicals, escaping from the primary cage, is determined as 0.28 ± 0.06 for the decay of the excited *trans*-azocumene and 0.18 ± 0.04 for the thermal cleavage of the *cis*-isomer. The self-termination of cumyl radicals proceeds with a rate constant $2k_t = (7 \pm 1) \cdot 10^8\ M^{-1}s^{-1}$ in benzene at RT.

1. Introduction

The electron spin system of reactive radicals in solution, as a rule, exhibits chemically induced dynamic electron polarization (CIDEP), which can arise from a variety of mechanisms like the triplet mechanism (TM), the radical pair mechanism (RPM), the radical-triplet pair mechanism (RTPM), or via electron-nuclear cross relaxation [1–3]. A large amount of information on these polarizations has been gathered during the past 25 years, and the CIDEP phenomenon has been utilized in numerous studies to get insights into details of radical generation and radical reactions. However, one of the basic physical quantities involved, the magnitudes of the induced polarizations, have remained unknown in the vast majority of investigations. As they are difficult to measure, accurate information about them is still scarce [1, 2, 4–8].

Usually, CIDEP studies employ time-resolved EPR measurements after pulse radiolytic or flash photolytic radical generation [8]. The EPR intensity in dependence

on time then contains all information about the spin dynamics as well as the chemical kinetics of the system and, therefore, is determined by a variety of parameters which are all more or less unknown. In one of the simplest cases already, when identical radicals are generated by flash photolysis and their magnetization is detected by time-resolved cw-EPR spectroscopy, at least eight parameters are influencing the time-profile, if the RPM only is operative: the initial concentration of radicals, their initial z-magnetization, their spin-lattice and spin-spin relaxation times, their rate constant for bimolecular termination, the polarization they gain in non-reactive encounters, as well as the amplitude of the resonant microwave field and the sensitivity factor of the EPR detection system. Evaluation of all these quantities via a multiparameter least-squares fit of the relevant Bloch type differential equations to the experimental data is a hopeless undertaking, as errors in the parameters are mutual compensating and the fits are anything but unequivocal, even if a few of the parameters can be measured separately or be taken from literature [6] and (Blättler C., Paul H., unpubl.). Moreover, previous investigations have shown, that the same experimental time-profile may be described about equally well even with different kinetic schemes and CIDEP mechanisms [9, 10]. Therefore, in order to evaluate accurate magnitudes of CIDEP from EPR time-profiles, as many as possible of the other parameters should be determined precisely in separate experiments, and, of course, the kinetics must be known. Though this is basically true for cw-EPR as well as FT-EPR detection, the problem seems to be less severe in the latter technique [6, 11, 12].

Under suitable conditions, the time-resolved cw-EPR (TREPR) signal after pulsed radical generation can show transient Torrey oscillations [13–15], and it is well known that their analysis, in principle, should yield several of the above mentioned parameters [8]. Hitherto, this possibility seems to have been exploited for CIDEP measurements only partially in a few investigations [16–19]. In this work, we report on a TREPR study of cumyl radicals, generated from *trans*-azocumene by laser flash photolysis. It is shown that analysis of Torrey oscillations, EPR time-profiles and lineshapes, as well as a sensitivity calibration of the EPR detection system, allows a complete determination of the kinetics, spin dynamics, and the magnitude of the CIDEP with good accuracy.

The photolysis of *trans*-azocumene (*t*AC) is a well defined, clean radical source and, therefore, an ideal model system. The following scheme gives the reaction sequence of *t*AC upon uv irradiation [20–22]:

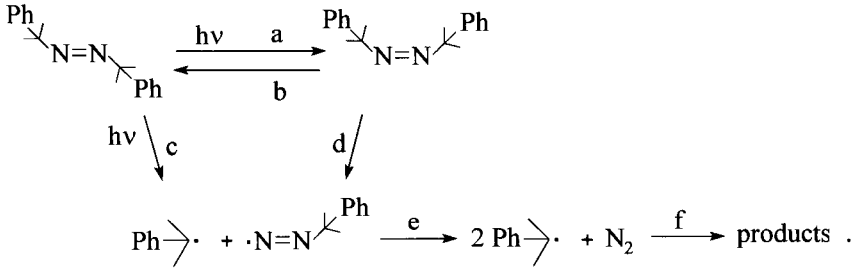

Direct photolysis (step c) and isomerization (step a) are the competing primary steps after excitation. The *cis*-isomer (*c*AC) decays by a kinetics of first order (steps b and d) with a mean lifetime of 5 μs at room temperature in cyclohexane solution [21]. The lifetime of the cumyldiazenyl radical (step e) is not exactly known, but an upper limit of less than 20 ns has been suggested [21]. In inert solvents the resulting cumyl radicals terminate in in-cage and out-of-cage processes to combination and disproportionation products [23, 24].

2. Experimental

Our experimental setup for time-resolved EPR measurements after laser flash photolytic radical generation has been described previously [25]. It comprises an Nd-YAG laser (355 nm, 6 ns pulse width) and a cw-EPR detection system without field modulation (80 ns response time). All experiments were carried out at room temperature with benzene solutions. After deoxygenation by purging with helium or argon, they were exposed to laser irradiation (5–15 mJ per pulse on sample surface, 10 Hz repetition rate) while slowly flowing (50–100 laser shots per irradiation volume) through a quartz cell (2 mm optical path length) inside a TE_{103} EPR cavity. To avoid large concentration gradients across the sample volume an initial *t*AC concentration of 27 mM (OD = 0.2) was chosen for all experiments. Sample depletion was controlled by absorption spectroscopy and kept below 20%. Spectra were recorded at microwave powers ranging from 0.1 to 100 mW. Steady-state EPR spectra and calibration experiments were performed on a commercial EPR-spectrometer (Bruker ESP300).

Trans-azocumene was synthesized as described by Stowell [26]. All other chemicals were purchased from Fluka and Aldrich in their purest commercially available forms and used as supplied.

3. Results

After laser flash irradiation of *t*AC ($\varepsilon_{355} = 37.3 \pm 0.1\ M^{-1}cm^{-1}$) in benzene solution, the EPR spectra given in Fig. 1 are observed. They are unambiguously assignable to the cumyl radical because of the hyperfine couplings 6H(CH_3): 1.623(1) mT, 2H(o): 0.476(1) mT, 2H(m): 0.161(1) mT, and H(p): 0.551(1) mT, which agree with literature data [27]. As the photolysis of *t*AC occurs from an excited singlet state, the spectrum at short times, Fig. 1a, exhibits an A/E polarization pattern due to the RPM in the geminate radical pair. At longer times, Fig. 1b, the F-pair polarization dominates, giving rise to an E/A multiplet polarization. No initial net polarization is observed, i.e., there is no noticeable geminate pair polarization due to the different *g*-values of the cumyl and diazenyl radical. This agrees well with previous CIDNP results on the photolysis of symmetric azoalkanes, which also did not find any nuclear polarization due to the primary unsymmetrical radical pair, indicating a lifetime of the diazenyl radical in the picosecond range [20].

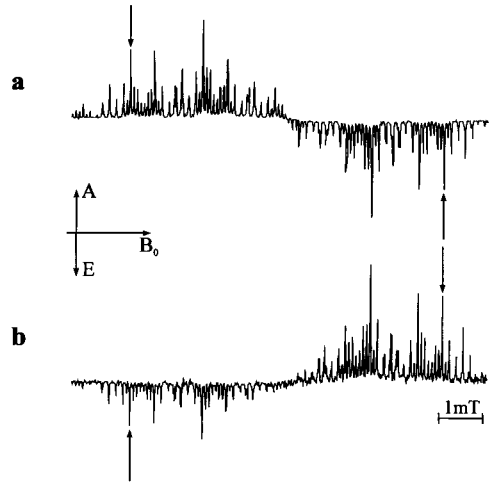

Fig. 1. Time-resolved EPR spectra of cumyl radicals generated by laser flash photolysis of *trans*-azocumene in benzene 3 μs (**a**) and 50 μs (**b**) after laser excitation. Spectrum **b** is given with eight times larger amplification than **a**. The high- and low-field resonance marked by arrows have been used for detailed analysis.

Two arrows in Fig. 1 mark a high- and low-field line positioned symmetrically to the center of the spectrum. Their overlap with neighboring resonances is negligibly weak and, therefore, their EPR time-profiles have been chosen to investigate the CIDEP and chemical kinetics of the radical system. The time-profiles on resonance of these two lines were analyzed in terms of Bloch equations, modified by additional terms to allow for chemical kinetics and electron spin polarization, as proposed by Pedersen [28] and Fessenden [16],

$$\frac{\mathrm{d}}{\mathrm{d}t}u = -T_2^{-1}u + \Delta\omega v \quad ,$$

$$\frac{\mathrm{d}}{\mathrm{d}t}v = -\Delta\omega u - T_2^{-1}v + \omega_1 M_z \quad ,$$

$$\frac{\mathrm{d}}{\mathrm{d}t}M_z = -\omega_1 v - T_1^{-1}M_z + f_a(t) \tag{1}$$

with

$$f_a(t) = T_1^{-1}P_{eq}[\mathrm{R}] + 2k_t[\mathrm{R}]^2 P_F P_{eq} + 2k_1\beta[c\mathrm{AC}]P_G P_{eq} \quad , \tag{2}$$

and

$$\frac{\mathrm{d}}{\mathrm{d}t}[\mathrm{R}] = -2k_t[\mathrm{R}]^2 + 2k_1\beta[c\mathrm{AC}] \quad ,$$

$$\frac{\mathrm{d}}{\mathrm{d}t}[c\mathrm{AC}] = -k_1[c\mathrm{AC}] \quad , \tag{3}$$

where u and v represent the perpendicular magnetization in the rotating frame, $\Delta\omega$ the offset from resonance, T_1 and T_2 the relaxation times, ω_1 the microwave magnetic field amplitude, [R] the cumyl radical concentration, P_{eq}[R] the equilibrium z-magnetization, and P_F the polarization factor for F-pair polarization (in units of the Boltzmann polarization P_{eq}). The last term on the right-hand side of Eq. (2) takes into account the production of z-magnetization due to thermal decay of cAC. There, P_G describes the polarization generated in the geminate pair, and β measures the fraction of thermal cAc decay, which leads to radicals. Regarding the initial condition, it is assumed that on the time-scale of the TREPR experiment the direct photolysis of tAC is yielding a cumyl radical ensemble with no initial perpendicular magnetization ($u(0) = v(0) = 0$) and an initial z-magnetization $M_z(0) = P_G P_{eq}$[R](0). The latter is determined by the generated radical concentration [R](0) and the polarization P_G, which these radicals gain via the RPM in the geminate pair. Finally, it is noted that the above modifications of the Bloch equations for chemical reaction and CIDEP are purely phenomenological. They are thought to hold as long as the chemical decay of the radical ensemble is slow in comparison with the spin relaxation time T_1 [28].

In what follows, we will first fix a variety of the parameters in Eqs. (1)–(3) via separate experiments, and will then determine the others by least square fits of the equations to the EPR time-profiles.

3.1. Transient Nutations and Linewidth Measurements

The solution of Eq. (1) is well known and has been presented several times [29]. For the on-resonance case ($\Delta\omega = 0$) it reads

$$v(t) = \frac{\omega_1}{\omega_T} M_z(0) \exp(-\sigma t) \cdot \sin \omega_T t + \frac{\omega_1}{\omega_T} f_a(t) \otimes \left(\exp(-\sigma t) \cdot \sin \omega_T t\right) \tag{4}$$

with

$$\sigma = \frac{1}{2}(T_1^{-1} + T_2^{-1}) \quad ,$$

$$\omega_T = \sqrt{\omega_1^2 - \frac{1}{4}(T_1^{-1} - T_2^{-1})^2} \quad . \tag{5}$$

The second term on the right-hand side of Eq. (4) involves all parameters of the system because of the convolution integral with $f_a(t)$. However, if $2|\omega_1| > > |1/T_1 - 1/T_2|$, the first term leads to transient nutations, which are determined by only the four parameters ω_1, T_1, T_2, and $M_z(0)$. As an example, Fig. 2a gives

two EPR time-profiles on resonance of the low-field line (marked in Fig. 1), taken at low and high microwave power. In the latter case, where above condition for $2|\omega_1|$ is fulfilled, the EPR signal appears essentially as an exponentially damped oscillation. Figure 2b shows both EPR time-profiles after Fourier transformation in the frequency space. There, the Torrey oscillations become separated from the slower chemical kinetics, involved in $f_a(t)$ of the second term in Eq. (4), and appear as a strong line at ω_T ($\approx$380 kHz in Fig. 2b). Analysis of position, amplitude, and shape of this line at different incident microwave powers, according to the first term on the right-hand side of Eq. (4), yielded $\sigma = (1/T_1 + 1/T_2)/2 = (3.5\pm0.2)\cdot 10^5\ s^{-1}$ and, for our experimental conditions, $\omega_1^2 = 2.86\cdot 10^{11}\ rad^2/s^2$ per 1 mW incident microwave power as well as $M_z(0) = P_G P_{eq}[R](0) = 0.38\pm \pm 0.01$ V for the investigated EPR transition at 10 mJ/pulse light intensity on probe. The results obtained for these three parameters at different microwave powers are shown in Fig. 3. The broken line drawn in Fig. 2b gives the nuta-

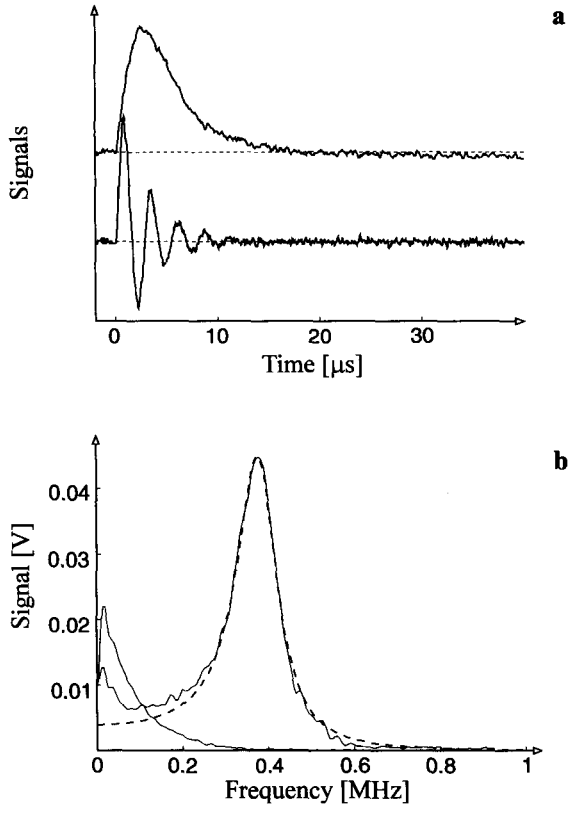

Fig. 2. Torrey oscillations. **a** Low-field EPR time-profiles after laser flash irradiation of *trans*-azocumene recorded at microwave powers 0.2 mW (upper trace) and 20 mW (lower trace). **b** Fourier transforms of the EPR time-profiles **a** and a simulation by Eq. (4) with neglect of the reaction term (broken line)

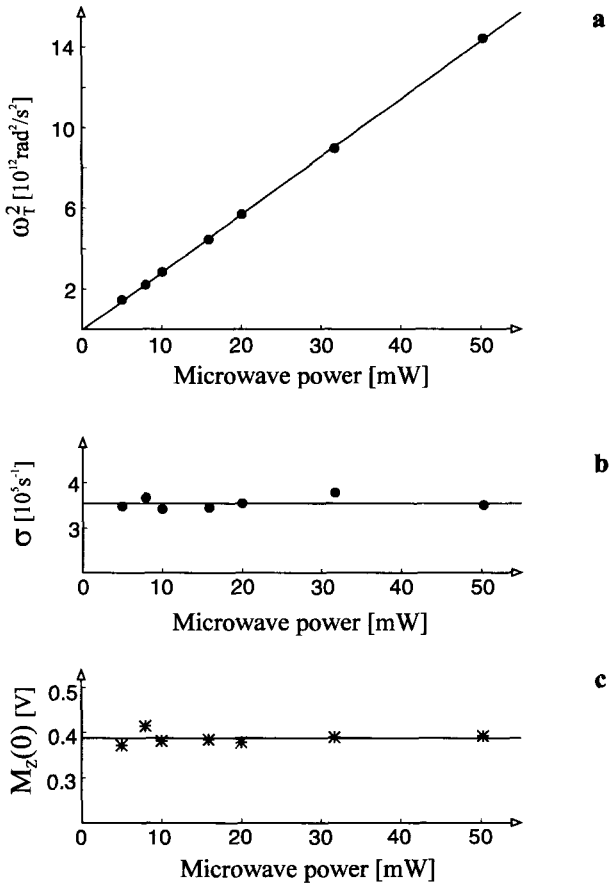

Fig. 3. **a** Evaluation of frequency, **b** exponential damping, and **c** amplitude of the Torrey oscillations at various microwave powers, via simulation of the Fourier transforms by Eq. (4) with neglect of the reaction term.

tions as calculated with the above parameters for the condition used in that experiment (20 mW incident microwave power).

It has to be mentioned that this simple evaluation of the Torrey oscillations in frequency space is an approximation, which requires the two terms on the right-hand side of Eq. (4) to be sufficiently separated. For this to be the case we found as adequate condition $\omega_T/4 \geq \sigma \geq 4\tau$, where τ denotes the mean chemical lifetime of the radicals. Another problem is associated with the second term in Eq. (4) in that it also contains a damped oscillation at the Torrey frequency ω_T. Fortunately, the amplitude of this oscillation is roughly proportional to $1/\omega_T$ [29], so that it can always be made small by increasing the microwave power. In our measurements its contribution was estimated to be negligibly small. We checked for this point once again at the end of the evaluation, when all the parameters of the

system were known (vide infra), by calculating the Fourier transform of Eq. (4) with and without its second term. The result, given in Fig. 4, clearly demonstrates the nutation line in frequency space to be nearly exclusively determined by the first term of Eq. (4). Finally, it is noted that all these analyses, of course, require the response function of the EPR detection system to be taken into account.

In principal, the spin-spin and spin-lattice relaxation times can also be obtained separately from the Torrey oscillations. However, we found it to be more convenient and accurate to use, besides the damping parameter σ, the linewidth in order to determine T_1 and T_2 separately. At times $t > 50$ μs, much longer than the relaxation times, the two EPR lines under investigation showed Lorentzian lineshapes with a dependence on the incident microwave power following

$$\Delta B_{1/2}^2 = (\Delta B_{1/2}^0)^2 (1 + \omega_1^2 T_1 T_2) \quad , \tag{6}$$

with $\Delta B_{1/2}^0 = 2/(\gamma T_2)$. Therefore, the linewidth $\Delta B_{1/2}$ at times 60 μs $< t <$ 100 μs was determined at various microwave powers, and the relaxation times were calculated from $2\sigma = 1/T_1 + 1/T_2$ and

$$\frac{1}{2}\sigma \Delta B_{1/2}^2 \gamma^2 T_2^3 - \left(\frac{1}{4}\Delta B_{1/2}^2 \gamma^2 + \omega_1^2\right) T_2^2 - 2\sigma T_2 + 1 = 0 \quad . \tag{7}$$

Taking into account the errors of the linewidth measurement, the numerical solution yielded $T_2 = 2.49 \pm 0.11$ μs and $T_1 = 3.5 \pm 0.3$ μs for cumyl radicals in benzene at room temperature.

Finally, we have checked the accuracy of the above results by analyzing a 2-cyano-2-propyl radical system (photolysis of AIBN in benzene at 355 nm) and

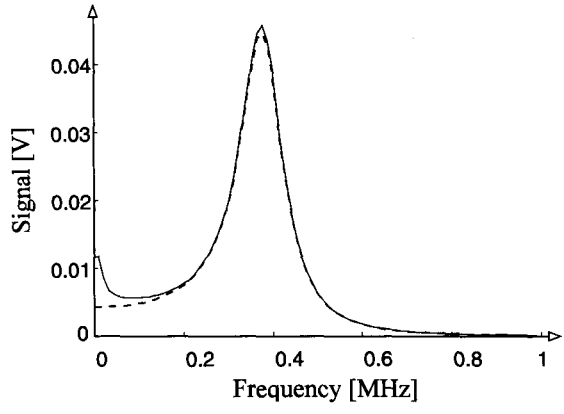

Fig. 4. Simulation of the Fourier transform of Torrey oscillations, observed at 20 mW microwave power, by Eq. (4) with (full line) and without (broken line) the reaction term.

the cumyl radical system, which is created after photolysis of dicumyl ketone (benzene, 308 nm). The values obtained for ω_1 differed by less than 2% from the above one, and in the latter system the same relaxation times as before were found for the cumyl radicals.

3.2. Equilibrium Polarization and Sensitivity Factor

A quantitative analysis of the EPR time-profiles requires determination of the sensitivity factor of the detection system. Multiplication of this factor with the equilibrium polarization allows a conversion of P_{eq} from its unit $(J \cdot T^{-1} \cdot M^{-1})$ into the unit of the measured signal voltage per radical concentration $(V \cdot M^{-1})$. Then, the Bloch equations can be used directly in units of the signal voltage.

In order to measure the sensitivity factor, separate EPR experiments were carried out with a solution of the persistent nitroxyl radical TEMPO (1 mM) in benzene. Its EPR spectrum consists of three lines due to the nitrogen hfs. The total EPR absorption of the sample is calculated from the Bloch equations as:

$$I_{\text{theor}} = \int_{-\infty}^{\infty} v(\omega)\,\mathrm{d}\omega = \pi M_z^0 \omega_1 = \pi P_{\text{eq}}^{\text{total}}[\text{TEMPO}]\omega_1 \quad . \tag{8}$$

In order to measure this total absorption, we have connected a sawtooth voltage to the Helmholtz coils of the resonator and have swept the B_0-field over one of the three TEMPO resonances within about 20 μs (the timescale of our time-resolved experiments). The experimental EPR absorption was then calculated from the observed maximum signal height according to

$$I_{\text{exp}} = \int_{-\infty}^{\infty} S(\omega)\,\mathrm{d}\omega = 3S_{\max}\,\Delta\omega_{1/2}\,\alpha \quad , \tag{9}$$

where $\Delta\omega_{1/2}$ and α are the width and lineshape factor, respectively, which have been derived from a careful simulation of the steady-state EPR spectrum of the TEMPO solution. Because of the proportionality $S = Cv$ we have $I_{\text{exp}} = CI_{\text{theor}}$ and hence $I_{\text{exp}}/(\pi\omega_1[\text{TEMPO}]) = CP_{\text{eq}}^{\text{total}}$ in [V/M] for the TEMPO experiment. For the TREPR experiment this factor has to be rescaled by taking into account the ratio of the irradiated volume and that of the TEMPO experiment, as well as the ω_1 distribution along the cell height in the cavity, yielding

$$C_{\text{TREPR}} P_{\text{eq}}^{\text{total}} = \frac{I_{\text{exp}}}{\pi\omega_1[\text{TEMPO}]} \cdot \frac{\delta w}{\Delta w} \cdot \frac{\int_{\pi(\Delta h-\delta h)/2\Delta h}^{\pi(\Delta h+\delta h)/2\Delta h} \sin^2 x\,\mathrm{d}x}{\int_0^{\pi} \sin^2 x\,\mathrm{d}x} \tag{10}$$

in [V/M] for the TREPR experiment. Here, δw, δh and Δw, Δh are width and height of the irradiated surface and the total cell surface in the cavity, respectively. From the errors of the measurements and geometrical determinations, and Eq. (10), we finally obtained $C_{\mathrm{TREPR}} P_{\mathrm{eq}}^{\mathrm{total}} = 64.5 \pm 3.1$ kV/M for our experimental arrangement. For the analysis of the two cumyl radical resonances under consideration, this number was multiplied with the relative weight 20/2048 of the two resonances in the cumyl radical EPR spectrum, because Eq. (10) refers to the z-component of the total Boltzmann polarization of all hfs states. The result, 630 ± 30 V/M, was used for P_{eq} in the analysis of the time-profiles by fitting them with Eqs. (1)–(3).

3.3. Reaction Rate Constants and Initial Transient Concentrations

After having determined ω_1, T_1, T_2, $M_z(0)$, and P_{eq}, the remaining unknown parameters of the system are the rate constants k_1 and $2k_t$, the initial radical concentration [R](0), as well as the parameter $\beta[c\mathrm{AC}](0)$ and the F-pair polarization P_{F}. A variety of data and restrictions with respect to some of these parameters can be found in the literature. A rate constant $k_1 = 2 \cdot 10^5\ \mathrm{s}^{-1}$ has been estimated for the decomposition of *cis*-azocumene in cyclohexane [21]. Thus, k_1 can only be varied around this value. For the self-termination of cumyl radicals, rate constants $2k_t = 1.6 \cdot 10^{10}\ \mathrm{M}^{-1}\mathrm{s}^{-1}$ [30] and $3.6 \cdot 10^8\ \mathrm{M}^{-1}\mathrm{s}^{-1}$ [31] have been reported. The first one is certainly too large, and the second one seems to be based on an incorrect kinetic scheme [21]. However, for a variety of radicals having similar structure and size as the cumyl radical, termination rate constants in the range $5 \cdot 10^8 < 2k_t < 9 \cdot 10^8\ \mathrm{M}^{-1}\mathrm{s}^{-1}$ are known [32] for solvents with viscosities comparable to that of benzene. Therefore, $2k_t$ was varied within this range only.

The initial concentrations [R](0) and $\beta[c\mathrm{AC}](0)$ as well as the F-pair polarization P_{F} were left as free fit parameters. In order to find reasonable starting values for the initial transient concentrations we have estimated the sum [R](0) + $\beta[c\mathrm{AC}](0)$ from the absorbed laser light intensity per sample volume, the known quantum yield 0.36 of nitrogen formation [33], and a probability of 0.4 for geminate cage recombination as reported by Nelsen and Bartlett [34]. In addition, we have checked our value for the absorbed laser light per sample volume, by measuring spectrophotometrically the depletion of *trans*-azocumene, from which we calculated a quantum yield of 0.37 ± 0.01, in good agreement with the above N_2 quantum yield.

3.4. Computer Simulations

The system of Eqs. (1)–(3) was numerically integrated, and the solution was fit with a SIMPLEX routine to the time-profiles of 20 high/low-field resonance line pairs (marked in Fig. 1), which had been taken at various microwave powers and laser light intensities. In each case, only the three parameters [R](0), $\beta[c\mathrm{AC}](0)$, and P_{F} were fit, but the procedure was repeated several times with different values

for k_1 and $2k_t$. It was also checked that the fits were unique by starting the SIMPLEX algorithm with different initial parameter sets. The best agreement with the experimental traces ($\chi^2_{red} = 1.2$) was found for the following parameter set: $2k_t = (7\pm1)\cdot10^8$ $M^{-1}s^{-1}$, $k_1 = (7.5\pm1)\cdot10^4$ s^{-1}, $P_F = 48\pm5$, and $P_G = 32\pm2$. The other parameters determined above, $\omega_1 = 5.35\cdot10^5$ rad/s per 1 mW, $T_1 = 3.5\pm0.3$ μs, $T_2 = 2.5\pm0.1$ μs, and $P_{eq} = 630\pm30$ V/M, were left unchanged, as their variation within the error limits did not improve the fits, but rather impaired them. It is this parameter set, which has been taken to calculate Fig. 4. A comparison of experimental time-profiles and their fits is shown in Fig. 5 for two different microwave powers. Finally, from the absorbed laser light, the initial radical concentration (≈20 μM for 10 mJ laser pulse energy on probe), and the quantity

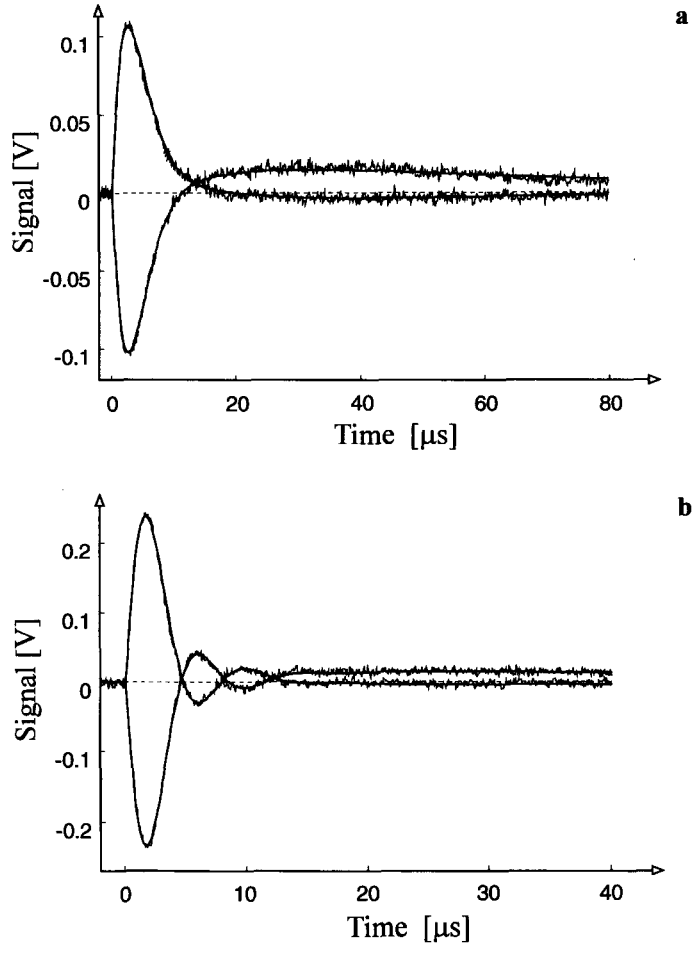

Fig. 5. High- and low-field EPR time-profiles of cumyl radicals after laser flash irradiation of *trans*-azocumene, recorded at microwave powers 0.2 mW (**a**) and 2 mW (**b**), as well as their simulations by Eqs. (1)–(3).

$\beta[c\mathrm{AC}](0)$ (≈ 7 μM at the same laser pulse energy) the quantum yield for free radicals, escaping from the primary cage, was estimated as 0.28 ± 0.06 for the decay of the excited *trans*-azocumene and 0.18 ± 0.04 for the thermal decay of the *cis*-isomer.

4. Discussion

The EPR time-profiles of the cumyl radicals, generated by photolysis of azocumene, involve ten unknown or not accurately known parameters, which determine the spin dynamics, the CIDEP, and the chemical kinetics of the system. All these parameters have been obtained with reasonable accuracy via a consequent analysis of the transient Torrey oscillations, a thorough sensitivity calibration of the EPR detection system, and least-square fits to the experimental traces. The analysis has profited mainly from the relatively long spin relaxation times T_1 and T_2 of cumyl radicals in benzene at RT. This allows a rather accurate evaluation of ω_1, T_1, T_2, and especially the crucial parameter $M_z(0)$. It also provides a good signal/noise ratio despite the intensity distribution on many resonances and the relatively low initial radical concentration, which is mandatory for an accurate separation of the Torrey oscillations from a slow chemical kinetics in frequency space. Another special feature of the system is its cleavage into radicals from a singlet molecular precursor, which results in opposite phases of the geminate and F-pair CIDEP and, hence, makes the time-profiles very sensitive to the magnitudes P_G and P_F. Therefore, it remains to be seen to what extent the analysis presented here can also be applied to other, less favorable photochemical systems.

4.1. Rate Constants and Quantum Yields

The rate constant $2k_t = (7 \pm 1) \cdot 10^8\ \mathrm{M^{-1}s^{-1}}$, which we have obtained for the self-termination of cumyl radicals in benzene at RT lies well in the expected range [32] and needs no further discussion. More interesting is the thermal decay rate of *cis*-azocumene, $k_1 = (7.5 \pm 1) \cdot 10^4\ \mathrm{s^{-1}}$. In a previous flash photolysis investigation, Boate and Scaiano [21] found a lifetime of ≈ 5 μs for the *cis*-isomer in cyclohexane at RT. The EPR time-profiles, which we obtained using benzene as solvent, turned out to be incompatible with such a short lifetime but rather yielded 14 μs. We have checked this point by taking EPR time-profiles after photolysis of azocumene in some other solvents and found that in benzene the thermal decay of *cis*-azocumene is definitely slower than in alkane solvents. The reason for this is not quite clear, nor, if the *cis-trans* isomerization, the cleavage, or both processes are affected by the solvent.

The quantum yields for free radical formation, 0.28 ± 0.06 for the decay of the excited *trans*-azocumene and 0.18 ± 0.04 for the thermal decay of the *cis*-isomer, are novel informations about the photochemistry of this molecule. For the direct photocleavage (step c in the scheme of the reaction sequence of *t*AC upon uv ir-

radiation, see Section 1) leading to free radicals, Boate and Scaiano [21] have estimated a quantum yield ≤ 0.1. Our value agrees with this estimate and substantiates it. Further it is noted that half the sum of both yields (0.23 ± 0.04) is in satisfactory agreement with the total nitrogen quantum yield 0.36 [33], reduced by 40% cage recombination [34].

4.2. Spin Polarizations from Geminate and F-Pairs

The CIDEP observed after photolysis of azocumene is generated during reencounter sequences of the radicals forming the geminate and F-pairs. It results from different hyperfine energies of the species and the exchange interaction between them, which mix and split, respectively, the singlet and triplet states of the pair. From the observed polarization pattern, a pure emission/absorption antiphase polarization, it can be concluded that under our conditions the radical pair mechanism (RPM) is dominated by S-T_0 mixing [1, 29]. The theoretical description of the polarization, created in this process, is well established [35–37]. Its predicted magnitude depends on several molecular parameters:

1. The diffusion coefficient $D_{rel} = D_1 + D_2$ for relative translational motion of the two radicals forming the pair.

2. A parameter $2Q_{ij} = \sum_n A_{1n} M_{1n}^i - \sum_m A_{2m} M_{2m}^j$ describing the S-T_0 mixing frequency, where M_{1n}^i is the magnetic quantum number of the nth nucleus of radical 1 in an overall nuclear spin state i and A_{1n} its isotropic hfs constant (M_{2m}^j and A_{2m} have the analogous meaning for radical 2).

3. The distance dependent exchange interaction $J(r)$ between the species, which causes the splitting of the S and T_0 states of the radical pair. It is assumed to be spherical symmetric and describable by $J(r) = J_0 \exp\{-\lambda(r - d)\}$, where d denotes the distance of closest approach of the species. The decay of J with inter-radical separation, measured by λ, is often specified by a distance $r_{ex} = 5 \ln 10 \cdot \lambda^{-1}$, within which J diminishes by five orders of magnitude. This distance is expected to lie in the range between $r_{ex} \approx d$ and $\approx 2d$. The exchange amplitude J_0 is unknown.

For two cumyl radicals a distance of closest approach of $d \approx 6.2$ Å can be estimated from their van der Waals volume [38], and a coefficient for relative translational diffusion of $D_{rel} = 2D_R \approx 2.4 \cdot 10^{-9}$ $m^2 s^{-1}$ from the Stokes-Einstein equation and the viscosity of benzene at RT. The values for Q_{ij} are known from the hyperfine splittings of this radical. With these parameters we have calculated the theoretically predicted F-pair polarization P_F for the two cumyl resonances under consideration as a weighted sum over all hyperfine states (Eq. (7.9c) in [35]). The result and the experimental value are compared in Fig. 6 in dependence on the exchange amplitude J_0.

The experimentally determined F-pair polarization with its error is represented by a shadowed bar and the theoretical predictions by several lines. Figures 6a and 6c refer to weak exchange ($J_0 < 10^{11}$ rad/s) for the cases $r_{ex} = d$ and $r_{ex} = 2d$, respec-

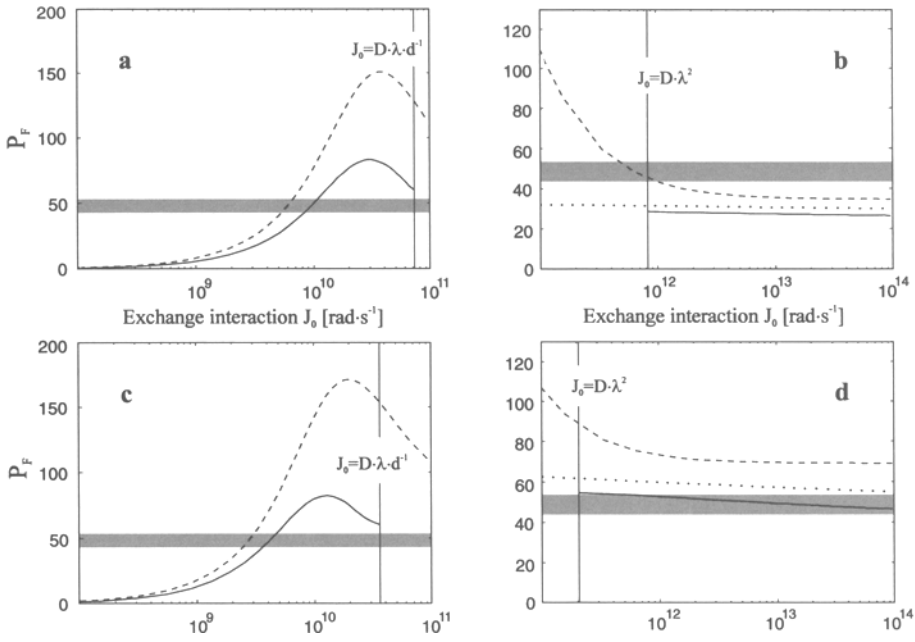

Fig. 6. Theoretical predictions for the F-pair polarization of cumyl radicals in benzene ($D_{rel} = 2.4 \cdot 10^{-9}$ m^{2}s^{-1}, $d = 6.2$ Å) in dependence on the exchange amplitude J_0. **a** Weak exchange limit ($J_0 \ll D\lambda d^{-1}$) and $r_{ex} = d$, according to Eq. (3.17) in [35] (dashed line) and Eq. (40) in [37] (solid line). **c** Dito, but for $r_{ex} = 2d$. **b** Strong exchange limit ($J_0 > D\lambda^2$) and $r_{ex} = d$, according to Eq. (3.17) in [35] (dashed line), Eq. (35) in [37] (solid line), and Eq. (21) in [36] (dotted line). **d** Dito, but for $r_{ex} = 2d$. The experimental value (shadowed bar) and the exchange interaction limits are also given.

tively, and Figs. 6b and 6d to strong exchange ($J_0 > 10^{11}$ rad/s) for the same two values of r_{ex}. The theoretical predictions have been calculated from different analytic approximations to the integral of the stochastic Liouville equation describing the RPM. The full lines in Fig. 6 are based on analytical results obtained by Shushin [37], which, for the regions $J_0 \ll D\lambda d^{-1}$ and $J_0 > D\lambda^2$, have been shown [39] to practically coincide with the exact numerical solution [35]. The dotted lines have been obtained from an approximation given by Adrian [36] for the strong exchange region. Finally, the broken lines in Fig. 6 are based on an equation proposed by Pedersen [35], which should qualitatively describe the magnitude of the F-pair polarization over the whole range of possible exchange amplitudes. Obviously, the CIDEP created in cumyl radical F-pairs in benzene is compatible with two interpretations. Either the exchange interaction is strong ($10^{12} < J_0 < 10^{14}$ rad/s) and decays with $r_{ex} \approx 2d$, or it is weak ($3 \cdot 10^9 < J_0 < 10^{10}$ rad/s) and decays with an r_{ex} between $r_{ex} \approx d$ and $\approx 2d$. To decide, which of both situations is true, needs additional information, e.g., the dependence of P_F on the diffusion coefficient. Experimental results on this dependence will be reported later.

A result of particular interest is the magnitude of the geminate pair polarization P_G in comparison to the F-pair polarization P_F. For the system investigated here,

the ratio of both polarizations turns out to be $|P_F/P_G| = 1.5 \pm 0.2$, i.e., the geminate polarization is definitely smaller than the F-pair one. As we have not observed any net emissive polarization, we believe that the geminate pair can be considered to be made up of two cumyl radicals, at least on the time scale the RPM is operative. Then, geminate and F-pairs are identical radical pairs under identical reaction conditions, except for a certain initial separation the radicals in the geminate pairs might have because of the nitrogen loss and/or the exothermicity of the cleavage reaction.

In a previous investigation [40], a ratio $|P_F/P_G| = 1$ has been measured for 2-propyl-2-ol radicals, generated by photoreduction of acetone with 2-propanol in aqueous solution. This reaction proceeds from the acetone triplet state, and for triplet geminate pairs the initial separation of the species hardly affects the evolution of CIDEP, as long as this separation remains within the exchange region. However, the situation changes drastically for singlet geminate pairs, for which a strong dependence of the CIDEP on the initial inter-radical distance would not be unexpected [39]. In fact, analysis of the geminate CIDEP in dependence on the viscosity and comparison with the cage recombination offers a unique possibility to get a clearer picture of the primary events and the initial distance distribution after the cleavage reaction of azoalkanes (Savitsky A.N., Paul H., Shushin A.I., unpubl.).

Acknowledgements

The authors thank I. Verhoolen for the preparation of *trans*-azocumene and product analyses, A. I. Shushin (Moscow) for helpful discussions, and gratefully acknowledge financial support by the Swiss National Foundation for Scientific Research. The investigation was undertaken in the frame of an INTAS project (93-1626-ext) on magnetic spin effects in chemical reaction.

References

[1] Salikhov K.M., Molin Yu.N., Sagdeev R.Z., Buchachenko A.L.: Spin Polarization and Magnetic Effects in Radical Reactions (Molin Yu.N., ed.). Amsterdam: Elsevier 1984.
[2] McLauchlan K.A., Yeung M.T.: Specialist Periodical Report "Electron Spin Resonance" **14**, 32–62 (1994)
[3] Goudsmit G.-H., Jent F., Paul H.: Z. Phys. Chem. **180**, 51–64 (1993)
[4] Trifunac A.D., Lawler R.G., Bartels D.M., Thurnauer M.C.: Prog. React. Kin. **14**, 45–156 (1986)
[5] Wan J.K.S., Depew M.C.: Res. Chem. Intermed. **18**, 227–292 (1992)
[6] van Willigen H., Levstein P.R., Ebersole M.H.: Chem. Rev. **93**, 173–197 (1993)
[7] Hirota N., Tominaga K., Yamauchi S.: Bull. Chem. Soc. Jpn. **68**, 2997–3010 (1995)
[8] McLauchlan K.A.: Modern Pulsed and Continuous-Wave Electron Spin Resonance (Kevan L., Bowman M.K., eds.), pp. 285–363. New York: John Wiley & Sons 1990.
[9] Blättler C., Paul H.: Res. Chem. Intermed. **16**, 201–211 (1991)
[10] Mukai M., Yamauchi S., Hirota N.: J. Phys. Chem. **96**, 3305–3311 (1992)
[11] Steren C.A., van Willigen H., Dinse K.-P.: J. Phys. Chem. **98**, 7464–7469 (1994)
[12] Shkrob I.A., Trifunac A.D.: Radiat. Phys. Chem. **46**, 83–96 (1995)
[13] Torrey H.C.: Phys. Rev. **76**, 1059–1068 (1949)
[14] Verma N.C., Fessenden R.W.: J. Chem. Phys. **58**, 2501–2506 (1973)

[15] Atkins P.W., Dobbs A.J., McLauchlan K.A.: Chem. Phys. Lett. **25**, 105–107 (1974)
[16] Verma N.C., Fessenden R.W.: J. Chem. Phys. **65**, 2139–2155 (1976)
[17] Beckert D., Mehler K.: Ber. Bunsenges. Phys. Chem. **87**, 587–591 (1983); *ibid.* **88**, 1013–1021 (1984)
[18] Beckert D., Fessenden R.W.: J. Phys. Chem. **100**, 1622–1629 (1996)
[19] McLauchlan K.A., Yeung M.T.: Mol. Phys. **89**, 1423–1443 (1996)
[20] Engel P.S.: Chem. Rev. **80**, 99–149 (1980)
[21] Boate D.R., Scaiano J.C.: Tetrahedron Lett. **30**, 4633–4636 (1989)
[22] Scott T.W., Doubleday C., Jr.: Chem. Phys. Lett. **178**, 9–18 (1990)
[23] Nelsen S.F., Barlett P.D.: J. Am. Chem. Soc. **88**, 137–143 (1966)
[24] Skinner K.J., Hochster H.S., McBride J.M.: J. Am. Chem. Soc. **96**, 4301–4306 (1974)
[25] Jent F., Paul H.: Chem. Phys. Lett. **160**, 632–639 (1989)
[26] Stowell J.C.: J. Org. Chem. **30**, 2360–2364 (1967)
[27] Landolt-Börnstein: Magnetic Properties of Free Radicals, New Series, Group II, v. 9b (Fischer H., Hellwege K.-H., eds.). Berlin: Springer 1977.
[28] Pedersen J.B.: J. Chem. Phys. **59**, 2656–2667 (1973)
[29] Hore P.J., Joslin C.G., McLauchlan K.A.: Specialist Periodical Report "Electron Spin Resonance" **5**, 1–45 (1979)
[30] Weiner S.A., Hammond G.S.: J. Am. Chem. Soc. **91**, 986–991 (1969)
[31] Sumiyoshi T., Kamachi M., Kuwae Y., Schnabel W.: Bull. Chem. Soc. Jpn. **60**, 77–81 (1987)
[32] Landolt-Börnstein: Radical Reaction Rates in Liquids, New Series, Group II, v. 13 (Fischer H., ed.). Berlin: Springer 1984; Landolt-Börnstein: Radical Reaction Rates in Liquids, New Series, Group II, v. 18 (Fischer H., ed.). Berlin: Springer 1994.
[33] Engel P.S., Steel C.: Acc. Chem. Res. **6**, 275–281 (1973)
[34] Nelsen S.F., Barlett P.D.: J. Am. Chem. Soc. **88**, 143–149 (1966)
[35] Freed J.H., Pedersen J.B.: Adv. Magn. Reson. **8**, 1–84 (1976)
[36] Adrian F.J.: Res. Chem. Intermed. **16**, 99–125 (1991)
[37] Shushin A.I.: Chem. Phys. **144**, 201–222, 223–239 (1990)
[38] Edward J.T.: J. Chem. Ed. **47**, 261–270 (1970)
[39] Shushin A.I., Pedersen J.B., Lolle L.I.: Chem. Phys. **177**, 119–131 (1993)
[40] Paul H.: Chem. Phys. **40**, 265–274 (1979); *ibid.* **43**, 294 (1979)

Author's address: Prof. Dr. H. Paul, Physikalisch-Chemisches Institut, Universität Zürich, Winterthurerstr. 190, CH-8057 Zürich, Switzerland